



# Lithium tetrachloridoaluminate, $\text{LiAlCl}_4$ : a new polymorph (*oP12*, *Pmn2*<sub>1</sub>) with $\text{Li}^+$ in tetrahedral interstices

Stephan W. Prömpfer and Walter Frank\*

Institut für Anorganische Chemie und Strukturchemie, Lehrstuhl II: Material- und Strukturforschung, Heinrich-Heine-Universität Düsseldorf, Universitätsstrasse 1, D-40225 Düsseldorf, Germany. \*Correspondence e-mail: wfrank@hhu.de

Received 27 July 2017

Accepted 25 August 2017

Edited by M. Weil, Vienna University of Technology, Austria

**Keywords:** crystal structure; polymorphism; lithium tetrachloridoaluminate.

**CCDC reference:** 1570829

**Supporting information:** this article has supporting information at journals.iucr.org/e

Dissolving lithium chloride and aluminium chloride in boiling *para*- or *meta*-xylene and keeping the colourless solution at room temperature led to crystal growth of a new modification of lithium tetrachloridoaluminate,  $\text{LiAlCl}_4$ , which represents a second modification (*oP12*, *Pmn2*<sub>1</sub>) of the ternary salt besides the long known monoclinic form [ $\text{LiAlCl}_4$ (*mP24*, *P2*<sub>1</sub>/*c*); Mairesse *et al.* (1977). *Cryst. Struct. Commun.* **6**, 15–18]. The crystal structures of both modifications can be described as slightly distorted hexagonal closest packings of chloride anions. While the lithium cations in  $\text{LiAlCl}_4$ (*mP24*) are in octahedral coordination and the aluminium and lithium ions in the solid of orthorhombic  $\text{LiAlCl}_4$  occupy tetrahedral interstices with site symmetries *m* and 1, respectively, the lithium cation site being half-occupied (defect wurtz-stannite-type structure). From differential scanning calorimetry (DSC) measurements, no evidence for a phase transition of the orthorhombic modification is found until the material melts at 148 °C ( $T_{\text{peak}} = 152$  °C). The melting point is nearly identical to the literature data for  $\text{LiAlCl}_4$ (*mP24*) [146 °C; Weppner & Huggins (1976). *J. Electrochem. Soc.* **124**, 35–38]. From the melts of both polymorphs, the monoclinic modification recrystallizes.

## 1. Chemical context

The series of known crystal structures of alkali metal tetrachloridoaluminates  $M\text{AlCl}_4$ , with *M* = Li (Mairesse *et al.*, 1977), Na (Baenziger, 1951), K (Mairesse *et al.*, 1978*a*), Rb (Mairesse *et al.*, 1979) and Cs (Gearhart *et al.*, 1975; Mairesse *et al.*, 1979) was completed about 40 years ago and comparative structural studies were made (Mairesse *et al.*, 1979; Meyer & Schwan, 1980). With respect to ionic conductivity, both solid lithium tetrachloridoaluminate [ $\text{LiAlCl}_4$ (*mP24*, *P2*<sub>1</sub>/*c*); Mairesse *et al.*, 1977] and melts of the salt were investigated (Weppner & Huggins, 1976, 1977). Besides the importance of common commercial lithium–thionyl chloride battery systems (Winter & Brodd, 2004), recently published studies on the conductivity of  $\text{LiAlCl}_4$  in dimethyl carbonate or mixtures with ethylene carbonate (Scholz *et al.*, 2015) indicate that the substance is of continuous interest. In the course of our ongoing studies on arene complexation of main group metals (Frank, 1990; Frank *et al.*, 1987, 1996; Frank & Wittmer, 1997; Kugel, 2004; Bredenhagen, 2014), we isolated a new polymorph of  $\text{LiAlCl}_4$ (*oP12*, *Pmn2*<sub>1</sub>) from mixtures of lithium chloride and aluminium chloride in boiling *para*- or *meta*-xylene, determined its crystal structure by single-crystal X-ray diffraction and unequivocally proved polymorphism of this ternary compound.

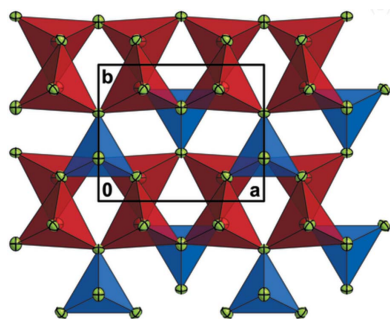


**Table 1**

Selected bond lengths (Å) in  $\text{LiAlCl}_4(oP12)$  and  $\text{LiAlCl}_4(mP24)$  (Perenthaler *et al.*, 1982) in the left and right column, respectively, and corresponding sums of bond orders, calculated using the Brown formalism ( $r_0 = 1.91$ ,  $B = 0.37$ ; Brese & O'Keeffe, 1991).

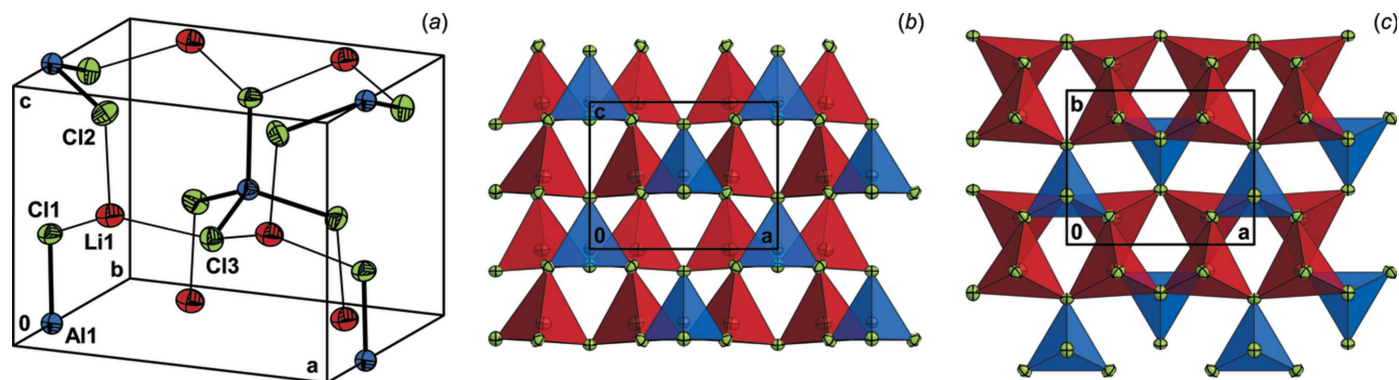
Li1—Cl1	2.322 (17)	Li—Cl1	2.475 (7)
Li1—Cl2	2.381 (21)	Li1—Cl2 <sup>x</sup>	2.729 (7)
Li1—Cl2 <sup>i</sup>	2.356 (14)	Li1—Cl2 <sup>xi</sup>	2.841 (7)
Li1—Cl3	2.413 (17)	Li1—Cl3	2.594 (7)
		Li1—Cl3 <sup>xii</sup>	2.769 (7)
		Li1—Cl4 <sup>xiii</sup>	2.493 (7)
$\Sigma_s(\text{Li—Cl})$	1.17	$\Sigma_s(\text{Li—Cl})$	0.87

Symmetry codes: (i)  $-x + \frac{1}{2}, -y, z - \frac{1}{2}$ ; (x)  $-x, y - \frac{1}{2}, -z + \frac{1}{2}$ ; (xi)  $x, -y + \frac{1}{2}, z + \frac{1}{2}$ ; (xii)  $-x, y - \frac{1}{2}, -z + \frac{1}{2}$ ; (xiii)  $1 - x, y - \frac{1}{2}, -z + \frac{1}{2}$ .

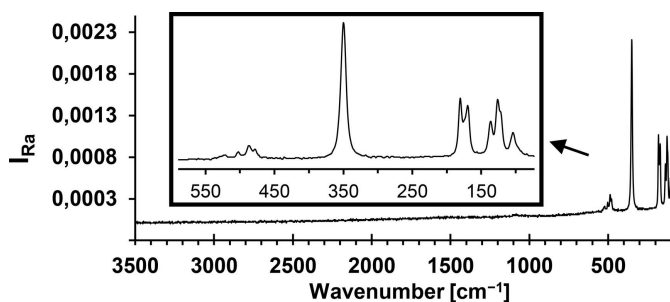
## 2. Structural commentary

$\text{LiAlCl}_4(oP12, Pmn2_1)$  crystallizes in a defect wurtz-stannite-type structure, an orthorhombic superstructure of the wurtzite-type structure, known from quaternary compounds of the type  $\text{Cu}_2M^{\text{II}}M^{\text{IV}}M_4^{\text{VI}}$  ( $M^{\text{II}} = \text{Mn, Fe, Co, Zn, Cd, Hg}$ ;  $M^{\text{IV}} = \text{Si, Ge, Sn}$ ;  $M^{\text{VI}} = \text{S, Se}$ ; except selenides of cobalt; Schäfer & Nitsche, 1977). The unit cell of the title compound contains four chloride anions and two aluminium cations, located in special positions (Wyckoff position 2a), as well as two lithium cations and another four chloride anions in general positions (4b), with the lithium site being half occupied, *i.e.* the asymmetric unit of the crystal structure is defined by half a tetrachloridoaluminate anion and one half-occupied lithium ion (Fig. 1a).

The crystal structures of the title compound, as well as of the monoclinic modification of lithium tetrachloridoaluminate, can be described as slightly distorted hexagonal closest packings of chloride anions. While the lithium cations in  $\text{LiAlCl}_4(mP24)$  are in octahedral coordination (Mairesse *et al.*, 1977), the aluminium and lithium ions in the solid of orthorhombic  $\text{LiAlCl}_4$  occupy tetrahedral interstices with site symmetries  $m$  and 1, respectively, the lithium cation site being half-occupied (Figs. 1b and 1c). Hence, the solid state of the title compound represents a three-dimensional network of


**Figure 1**

(a) The unit cell of the crystal structure of the title compound, with displacement ellipsoids drawn at the 50% probability level; (b) a view of the crystal structure in polyhedral representation perpendicular to a stacking direction ([101]) of the slightly distorted hexagonal closest packing of chloride anions; (c) a view of the crystal structure along [001].


**Figure 2**

Raman spectrum of the title compound.

corner-sharing tetrahedra, while in  $\text{LiAlCl}_4(mP24)$ , the octahedral and tetrahedral polyhedra are connected *via* corners as well as edges.  $\text{LiAlCl}_4(oP12)$  exhibits, as expected, shorter Li—Cl bonds (coordination number 4) as compared to corresponding bonds in monoclinic  $\text{LiAlCl}_4$  (coordination number 6). Using the Brown formalism (Brown & Altermatt, 1985), in both cases, bond orders which differ significantly from the expected value in view of the monovalent cation are computed (Table 1). In the case of orthorhombic  $\text{LiAlCl}_4$ , the strong deviation is based on the statistical disorder mentioned above and corresponding averaged geometric parameters obtained for occupied and non-occupied tetrahedral interstices, leading to higher Li—Cl bond orders in view of the exponential relationship between bond length and bond order.

## 3. Raman spectra

Raman bands in the vibrational spectrum of the title compound (Fig. 2) can be assigned to the four normal modes of vibration of a five atomic tetrahedral moiety of composition  $\text{AX}_4$  (Nakamoto, 1986)  $\nu_s(A_1)$ : 350  $\text{cm}^{-1}$ ,  $\delta_d(E)$ : 136 and 126  $\text{cm}^{-1}$ ,  $\nu_d(F_2)$ : 523, 502, 487 and 478  $\text{cm}^{-1}$  and  $\delta_d(F_2)$ : 180 and 170  $\text{cm}^{-1}$ . As in the Raman spectra of other alkali metal tetrachloridoaluminates (Rytter & Øye, 1973; Rubbens *et al.*, 1978) or  $\text{NH}_4\text{AlCl}_4$  (Mairesse *et al.*, 1978b), splitting of the bands is observed corresponding to the site effect and perturbation of the ideal tetrahedral symmetry of free  $\text{AlCl}_4^-$  anions caused by cation interactions.

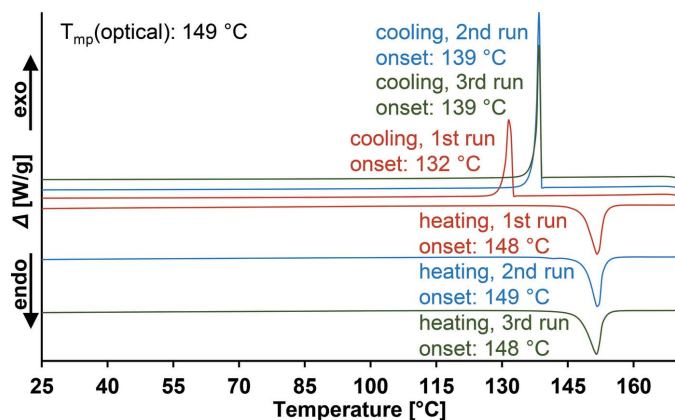


Figure 3  
DSC curves of multiple runs of the title compound.

#### 4. Thermal analysis and X-ray powder diffraction

From DSC measurements of the title compound (Fig. 3), no evidence for a phase transition is found until the material melts at 148 °C ( $T_{\text{peak}} = 152$  °C). The melting point is nearly identical to literature data for  $\text{LiAlCl}_4(mP24)$  (146 °C; Weppner & Huggins, 1976), which seems to be the only modification that recrystallizes from the melts of both modifications. This is demonstrated by high-quality X-ray powder diffraction patterns of the title compound, crystallized from *para*-xylene solution, and of the crystalline solid obtained by recrystallization from the melt (Fig. 4). In view of the current data, we suppose  $\text{LiAlCl}_4(oP12)$  to represent a metastable phase of lithium tetrachloridoaluminate whose melting point probably is nearly identical to that of monoclinic  $\text{LiAlCl}_4$  because it is very unlikely that a phase transition would not

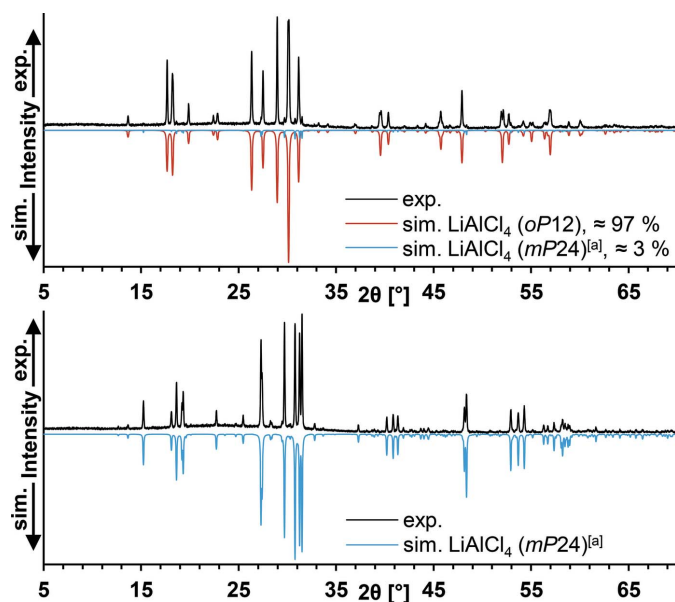


Figure 4  
X-ray powder diffraction pattern of the title compound before (top) and after (bottom) melting and corresponding simulations. [a] Single-crystal data for  $\text{LiAlCl}_4(mP24)$  are taken from the literature (Perenthaler *et al.*, 1982).

Table 2  
Experimental details.

Crystal data	$\text{LiAlCl}_4$
Chemical formula	175.72
$M_r$	Orthorhombic, $Pmn2_1$
Crystal system, space group	173
Temperature (K)	7.8273 (10), 6.4466 (10), 6.1304 (8)
$a, b, c$ (Å)	309.34 (7)
$V$ (Å <sup>3</sup> )	2
$Z$	Mo $K\alpha$
Radiation type	1.90
$\mu$ (mm <sup>-1</sup> )	0.65 × 0.10 × 0.03
Crystal size (mm)	
Data collection	Stoe IPDS 2T
Diffractometer	Multi-scan ( <i>X-AREA</i> ; Stoe & Cie, 2009)
Absorption correction	0.431, 0.583
$T_{\text{min}}, T_{\text{max}}$	3388, 880, 870
No. of measured, independent and observed [ $I > 2\sigma(I)$ ] reflections	0.092
$R_{\text{int}}$	0.685
$(\sin \theta/\lambda)_{\text{max}}$ (Å <sup>-1</sup> )	
Refinement	
$R[F^2 > 2\sigma(F^2)], wR(F^2), S$	0.028, 0.075, 1.21
No. of reflections	880
No. of parameters	37
No. of restraints	1
$\Delta\rho_{\text{max}}, \Delta\rho_{\text{min}}$ (e Å <sup>-3</sup> )	0.48, -0.46
Absolute structure	Flack $x$ determined using 386 quotients $[(I^+) - (I^-)] / [(I^+) + (I^-)]$ (Parsons <i>et al.</i> , 2013)
Absolute structure parameter	0.1 (2)

Computer programs: *X-AREA* (Stoe & Cie, 2009), *SHELXT* (Sheldrick, 2015a), *SHELXL2014* (Sheldrick, 2015b), *DIAMOND* (Brandenburg, 2016) and *pubCIF* (Westrip, 2010).

have been observed with the chosen DSC methods. The lower density of orthorhombic  $\text{LiAlCl}_4$  (1.89 g cm<sup>-3</sup>) compared to monoclinic  $\text{LiAlCl}_4$  (1.98 g cm<sup>-3</sup>; Mairesse *et al.*, 1979) supports the assumption of its metastability.

#### 5. Synthesis and crystallization

All sample preparations and manipulations were carried out in an atmosphere of dry argon (argon 5.0) using either Schlenk techniques or an MBraun LABstar glove-box. LiCl (beads, 99.9+%, anhydrous) and  $\text{AlCl}_3$  (powder, 99.99%) were purchased from Sigma–Aldrich and while LiCl was used as received,  $\text{AlCl}_3$  was first overlaid with elemental aluminium (grit, ≥97%, Sigma–Aldrich) and sublimed in a sealed ampoule in *vacuo* at 190 °C. *p*-Xylene (99%, Sigma–Aldrich) and *m*-xylene (99%, TCI) were refluxed with aluminium chloride, washed with 0.2 M NaOH, as well as distilled water, and distilled on molecular sieve 4 Å afterwards. In a typical reaction, 0.112 g (2.64 mmol) lithium chloride and 0.268 g (2.01 mmol) aluminium chloride were treated with 5 ml *p*-xylene and the mixture was refluxed for 30 min. Separation of the warm colourless solution from residual LiCl and removal of 4 ml of the solvent under reduced pressure at room temperature led to the formation of colourless crystals of the title compound.  $\text{LiAlCl}_4(oP12, Pmn2_1)$  was isolated in 60%

yield after washing the crystalline material with *p*-xylene and drying the solid in *vacuo* at room temperature.

The FT-Raman spectrum was recorded using a Bruker MultiRam spectrometer (*OPUS*; Bruker, 2006) equipped with an RT-InGaAs-detector and an Nd:YAG-Laser at 1064 nm (Stokes: 3500–70 cm<sup>-1</sup>; resolution: 2 cm<sup>-1</sup>):  $\nu_d(F_2, AlCl_4^-)$ : 523 (*w*), 502 (*w*), 487 (*m*), 478 (*w*);  $\nu_s(A_1, AlCl_4^-)$ : 350 (*vs*);  $\delta_d(F_2, AlCl_4^-)$ : 180 (*s*), 170 (*s*);  $\delta_d(E, AlCl_4^-)$ : 136 (*m*), 126 (*s*), 104 (*m*).

Thermal analysis (differential scanning calorimetry) was carried out with a Mettler Toledo DSC 1 calorimeter (*STARe*; Mettler-Toledo, 2008) equipped with an FRS 5 sensor using medium pressure steel crucibles without sealing rings. Measurements were carried out in an atmosphere of dry nitrogen at a heating/cooling rate of 5 °C min<sup>-1</sup> between 0 and 170 °C. First measurement heating:  $T_{onset} = 148$  °C ( $T_{peak} = 152$  °C), endothermic, melting; first measurement cooling:  $T_{onset} = 132$  °C ( $T_{peak} = 132$  °C), exothermic, crystallization; second measurement heating:  $T_{onset} = 149$  °C ( $T_{peak} = 152$  °C), endothermic, melting; second measurement cooling:  $T_{onset} = 139$  °C ( $T_{peak} = 138$  °C), exothermic, crystallization; third measurement heating:  $T_{onset} = 148$  °C ( $T_{peak} = 152$  °C), endothermic, melting; third measurement cooling:  $T_{onset} = 139$  °C ( $T_{peak} = 139$  °C), exothermic, crystallization. An alternative melting-point determination was carried out with a Mettler Toledo MP 90 Melting Point System:  $T_{mp} = 149$  °C.

X-ray powder diffraction patterns were measured using a Stoe & Cie STADI P (*WinXPOW*; Stoe & Cie, 2003) Debye-Scherrer diffractometer working in transmission mode with Cu  $K\alpha_1$  radiation [Ge(111) monochromator]. Simulations of powder patterns from single-crystal data were carried out using the computer program *PowderCell* (Kraus & Nolze, 2000).

## 6. Refinement

Crystal data, data collection and structure refinement details are summarized in Table 2. The lithium cation site (general position, Wyckoff site 4*b*) is half occupied.

## Acknowledgements

We thank E. Hammes and P. Roloff for technical support.

## References

Baenziger, N. C. (1951). *Acta Cryst.* **4**, 216–219.

- Brandenburg, K. (2016). *DIAMOND*. Crystal Impact GbR, Bonn, Germany.
- Bredenhagen, B. (2014). *Strukturchemische Untersuchungen an Systemen der Typen BiCl<sub>3</sub>/Aren und BiCl<sub>3</sub>/AlCl<sub>3</sub>/Aren*. Aachen: Shaker Verlag GmbH.
- Brese, N. E. & O'Keeffe, M. (1991). *Acta Cryst.* **B47**, 192–197.
- Brown, I. D. & Altermatt, D. (1985). *Acta Cryst.* **B41**, 244–247.
- Bruker (2006). *OPUS*. Bruker Optik GmbH, Ettlingen, Germany.
- Frank, W. (1990). *Z. Anorg. Allg. Chem.* **585**, 121–141.
- Frank, W., Korrell, G. & Reiss, G. J. (1996). *J. Organomet. Chem.* **506**, 293–300.
- Frank, W., Weber, J. & Fuchs, E. (1987). *Angew. Chem. Int. Ed. Engl.* **26**, 74–75.
- Frank, W. & Wittmer, F.-G. (1997). *Chem. Ber.* **130**, 1731–1732.
- Gearhart, R. C. Jr, Beck, J. D. & Wood, R. H. (1975). *Inorg. Chem.* **14**, 2413–2416.
- Kraus, W. & Nolze, G. (2000). *PowderCell*. Federal Institute for Materials Research and Testing, Berlin, Germany.
- Kugel, B. (2004). PhD thesis, Heinrich-Heine-Universität, Düsseldorf, Germany.
- Mairesse, G., Barbier, P. & Wignacourt, J.-P. (1977). *Cryst. Struct. Commun.* **6**, 15–18.
- Mairesse, G., Barbier, P. & Wignacourt, J.-P. (1978*a*). *Acta Cryst.* **B34**, 1328–1330.
- Mairesse, G., Barbier, P. & Wignacourt, J.-P. (1979). *Acta Cryst.* **B35**, 1573–1580.
- Mairesse, G., Barbier, P., Wignacourt, J.-P., Rubbens, A. & Wallart, F. (1978*b*). *Can. J. Chem.* **56**, 764–771.
- Mettler-Toledo (2008). *STARe*. Mettler-Toledo AG, Schwerzenbach, Switzerland.
- Meyer, G. & Schwan, E. (1980). *Z. Naturforsch. Teil B*, **35**, 117–118.
- Nakamoto, K. (1986). *Infrared and Raman Spectra of Inorganic and Coordination Compounds*, pp. 130–137. New York: John Wiley & Sons.
- Parsons, S., Flack, H. D. & Wagner, T. (2013). *Acta Cryst.* **B69**, 249–259.
- Perenthaler, E., Schulz, H. & Rabenau, A. (1982). *Z. Anorg. Allg. Chem.* **491**, 259–265.
- Rubbens, A., Wallart, F., Barbier, P., Mairesse, G. & Wignacourt, J.-P. (1978). *J. Raman Spectrosc.* **7**, 249–253.
- Rytter, E. & Øye, H. A. (1973). *J. Inorg. Nucl. Chem.* **35**, 4311–4313.
- Schäfer, W. & Nitsche, R. (1977). *Z. Kristallogr.* **145**, 356–370.
- Scholz, F., Unkrig, W., Eiden, P., Schmidt, M. A., Garsuch, A. & Krossing, I. (2015). *Eur. J. Inorg. Chem.* 3128–3138.
- Sheldrick, G. M. (2015*a*). *Acta Cryst.* **A71**, 3–8.
- Sheldrick, G. M. (2015*b*). *Acta Cryst.* **C71**, 3–8.
- Stoe & Cie (2003). *WinXPOW*. Stoe & Cie GmbH, Darmstadt, Germany.
- Stoe & Cie (2009). *X-AREA*. Stoe & Cie GmbH, Darmstadt, Germany.
- Weppner, W. & Huggins, R. A. (1976). *Phys. Lett. A*, **58**, 245–248.
- Weppner, W. & Huggins, R. A. (1977). *J. Electrochem. Soc.* **124**, 35–38.
- Westrip, S. P. (2010). *J. Appl. Cryst.* **43**, 920–925.
- Winter, M. & Brodd, R. J. (2004). *Chem. Rev.* **104**, 4245–4269.

## supporting information

*Acta Cryst.* (2017). E73, 1426-1429 [https://doi.org/10.1107/S205698901701235X]

## Lithium tetrachloridoaluminate, $\text{LiAlCl}_4$ : a new polymorph (*oP12*, *Pmn2*<sub>1</sub>) with $\text{Li}^+$ in tetrahedral interstices

Stephan W. Prömper and Walter Frank

### Computing details

Data collection: *X-AREA* (Stoe & Cie, 2009); cell refinement: *X-AREA* (Stoe & Cie, 2009); data reduction: *X-AREA* (Stoe & Cie, 2009); program(s) used to solve structure: *SHELXT* (Sheldrick, 2015a); program(s) used to refine structure: *SHELXL2014* (Sheldrick, 2015b); molecular graphics: *DIAMOND* (Brandenburg, 2016); software used to prepare material for publication: *publCIF* (Westrip, 2010).

### Lithium tetrachloridoaluminate

#### Crystal data

$\text{LiAlCl}_4$	$D_x = 1.887 \text{ Mg m}^{-3}$
$M_r = 175.72$	Mo $K\alpha$ radiation, $\lambda = 0.71073 \text{ \AA}$
Orthorhombic, <i>Pmn2</i> <sub>1</sub>	Cell parameters from 6814 reflections
$a = 7.8273 (10) \text{ \AA}$	$\theta = 3.0\text{--}29.7^\circ$
$b = 6.4466 (10) \text{ \AA}$	$\mu = 1.90 \text{ mm}^{-1}$
$c = 6.1304 (8) \text{ \AA}$	$T = 173 \text{ K}$
$V = 309.34 (7) \text{ \AA}^3$	Needle-shaped, colorless
$Z = 2$	$0.65 \times 0.10 \times 0.03 \text{ mm}$
$F(000) = 168$	

#### Data collection

Stoe IPDS 2T diffractometer	880 independent reflections
Radiation source: fine-focus sealed tube	870 reflections with $I > 2\sigma(I)$
$\varphi$ -scans	$R_{\text{int}} = 0.092$
Absorption correction: multi-scan ( <i>X-AREA</i> ; Stoe & Cie, 2009)	$\theta_{\text{max}} = 29.1^\circ$ , $\theta_{\text{min}} = 3.2^\circ$
$T_{\text{min}} = 0.431$ , $T_{\text{max}} = 0.583$	$h = -10 \rightarrow 10$
3388 measured reflections	$k = -8 \rightarrow 8$
	$l = -8 \rightarrow 8$

#### Refinement

Refinement on $F^2$	$w = 1/[\sigma^2(F_o^2) + (0.022P)^2 + 0.166P]$
Least-squares matrix: full	where $P = (F_o^2 + 2F_c^2)/3$
$R[F^2 > 2\sigma(F^2)] = 0.028$	$(\Delta/\sigma)_{\text{max}} < 0.001$
$wR(F^2) = 0.075$	$\Delta\rho_{\text{max}} = 0.48 \text{ e \AA}^{-3}$
$S = 1.21$	$\Delta\rho_{\text{min}} = -0.46 \text{ e \AA}^{-3}$
880 reflections	Absolute structure: Flack $x$ determined using
37 parameters	386 quotients $[(I^+)-(I^-)]/[(I^+)+(I^-)]$ (Parsons <i>et al.</i> , 2013)
1 restraint	Absolute structure parameter: 0.1 (2)

*Special details*

**Geometry.** All esds (except the esd in the dihedral angle between two l.s. planes) are estimated using the full covariance matrix. The cell esds are taken into account individually in the estimation of esds in distances, angles and torsion angles; correlations between esds in cell parameters are only used when they are defined by crystal symmetry. An approximate (isotropic) treatment of cell esds is used for estimating esds involving l.s. planes.

*Fractional atomic coordinates and isotropic or equivalent isotropic displacement parameters ( $\text{\AA}^2$ )*

	<i>x</i>	<i>y</i>	<i>z</i>	$U_{\text{iso}}^*/U_{\text{eq}}$	Occ. (<1)
Li1	0.246 (2)	0.1671 (19)	0.493 (3)	0.035 (3)	0.5
Cl1	0.0000	0.31452 (19)	0.34835 (19)	0.0305 (3)	
Cl2	0.22483 (12)	0.18042 (11)	0.88033 (12)	0.0317 (2)	
Cl3	0.5000	0.35454 (16)	0.3896 (3)	0.0295 (3)	
Al1	0.0000	0.3312 (2)	−0.0004 (3)	0.0229 (3)	

*Atomic displacement parameters ( $\text{\AA}^2$ )*

	$U^{11}$	$U^{22}$	$U^{33}$	$U^{12}$	$U^{13}$	$U^{23}$
Li1	0.043 (8)	0.033 (6)	0.029 (8)	0.001 (6)	0.002 (6)	0.000 (4)
Cl1	0.0300 (5)	0.0405 (6)	0.0208 (7)	0.000	0.000	0.0010 (4)
Cl2	0.0313 (4)	0.0314 (4)	0.0324 (5)	0.0078 (3)	0.0067 (5)	0.0017 (5)
Cl3	0.0300 (5)	0.0226 (4)	0.0360 (6)	0.000	0.000	−0.0055 (6)
Al1	0.0244 (8)	0.0212 (6)	0.0233 (8)	0.000	0.000	0.0008 (5)

*Geometric parameters ( $\text{\AA}$ ,  $^\circ$ )*

Li1—Cl1	2.322 (17)	Cl2—Li1 <sup>iv</sup>	2.356 (14)
Li1—Cl2 <sup>i</sup>	2.356 (14)	Cl3—Al1 <sup>v</sup>	2.1354 (18)
Li1—Cl2	2.38 (2)	Cl3—Li1 <sup>vi</sup>	2.413 (17)
Li1—Cl3	2.413 (17)	Al1—Cl3 <sup>vii</sup>	2.1354 (18)
Cl1—Al1	2.1404 (19)	Al1—Cl2 <sup>viii</sup>	2.1392 (11)
Cl1—Li1 <sup>ii</sup>	2.322 (17)	Al1—Cl2 <sup>ix</sup>	2.1392 (11)
Cl2—Al1 <sup>iii</sup>	2.1392 (11)		
Cl1—Li1—Cl2 <sup>i</sup>	111.0 (7)	Li1 <sup>iv</sup> —Cl2—Li1	104.6 (5)
Cl1—Li1—Cl2	108.0 (7)	Al1 <sup>v</sup> —Cl3—Li1 <sup>vi</sup>	113.1 (4)
Cl2 <sup>i</sup> —Li1—Cl2	109.5 (6)	Al1 <sup>v</sup> —Cl3—Li1	113.1 (4)
Cl1—Li1—Cl3	112.2 (6)	Li1 <sup>vi</sup> —Cl3—Li1	111.1 (7)
Cl2 <sup>i</sup> —Li1—Cl3	108.6 (7)	Cl3 <sup>vii</sup> —Al1—Cl2 <sup>viii</sup>	108.85 (6)
Cl2—Li1—Cl3	107.5 (7)	Cl3 <sup>vii</sup> —Al1—Cl2 <sup>ix</sup>	108.85 (6)
Al1—Cl1—Li1 <sup>ii</sup>	113.7 (5)	Cl2 <sup>viii</sup> —Al1—Cl2 <sup>ix</sup>	110.70 (8)
Al1—Cl1—Li1	113.7 (5)	Cl3 <sup>vii</sup> —Al1—Cl1	111.28 (9)
Li1 <sup>ii</sup> —Cl1—Li1	111.9 (9)	Cl2 <sup>viii</sup> —Al1—Cl1	108.58 (6)
Al1 <sup>iii</sup> —Cl2—Li1 <sup>iv</sup>	114.3 (4)	Cl2 <sup>ix</sup> —Al1—Cl1	108.58 (6)
Al1 <sup>iii</sup> —Cl2—Li1	114.4 (4)		

Symmetry codes: (i)  $-x+1/2, -y, z-1/2$ ; (ii)  $-x, y, z$ ; (iii)  $x, y, z+1$ ; (iv)  $-x+1/2, -y, z+1/2$ ; (v)  $-x+1/2, -y+1, z+1/2$ ; (vi)  $-x+1, y, z$ ; (vii)  $-x+1/2, -y+1, z-1/2$ ; (viii)  $-x, y, z-1$ ; (ix)  $x, y, z-1$ .